

Accepted Manuscript

Design, synthesis and molecular modeling of aloe-emodin derivatives as potent xanthine oxidase inhibitors

Da-Hua Shi, Wei Huang, Chao Li, Yu-Wei Liu, Shi-Fan Wang



PII: S0223-5234(14)00104-4

DOI: [10.1016/j.ejmech.2014.01.058](https://doi.org/10.1016/j.ejmech.2014.01.058)

Reference: EJMECH 6711

To appear in: *European Journal of Medicinal Chemistry*

Received Date: 17 March 2013

Revised Date: 23 January 2014

Accepted Date: 28 January 2014

Please cite this article as: D.-H. Shi, W. Huang, C. Li, Y.-W. Liu, S.-F. Wang, Design, synthesis and molecular modeling of aloe-emodin derivatives as potent xanthine oxidase inhibitors, *European Journal of Medicinal Chemistry* (2014), doi: 10.1016/j.ejmech.2014.01.058.

This is a PDF file of an unedited manuscript that has been accepted for publication. As a service to our customers we are providing this early version of the manuscript. The manuscript will undergo copyediting, typesetting, and review of the resulting proof before it is published in its final form. Please note that during the production process errors may be discovered which could affect the content, and all legal disclaimers that apply to the journal pertain.

GRAPHIC ABSTRACT

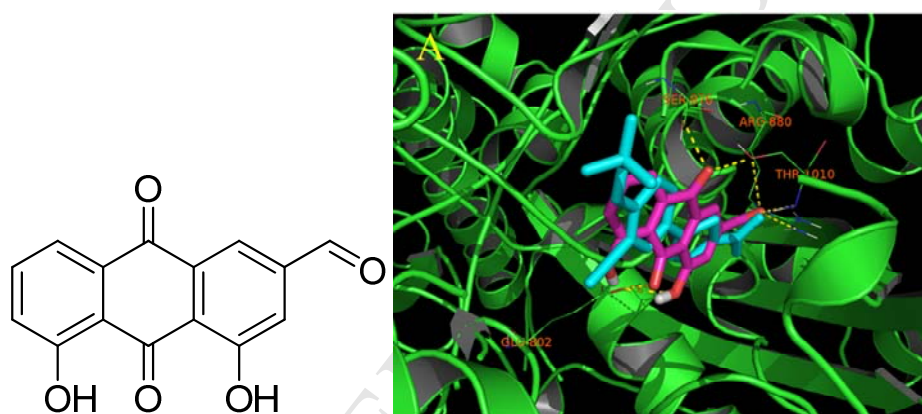
Design, synthesis and molecular modeling of aloe-emodin derivatives as potent xanthine oxidase inhibitors

Da-Hua Shi^{a,b}, Wei Huang^a, Chao Li^a, Yu-Wei Liu^c, Shi-Fan Wang^{a,*}

^a School of Ocean, Hainan University, Haikou 570228, People's Republic of China

^b School of Chemical Engineering, Huaihai Institute of Technology, Lianyungang 222005, People's Republic of China

^c Marine Economic Research Center of Jiangsu, Huaihai Institute of Technology, Lianyungang 222005, People's Republic of China



The structure of compound **A1** and the expected interaction between compound **A1** and the binding site of XDH (PDB NO. 1VDV)

* Address for Correspondence: School of Ocean, Hainan University, Haikou 570228, People's Republic of China, E-mail: wangsf777@163.com

- We designed and synthesized a series of aloe-emodin derivatives.
- We evaluated the xanthine oxidase-inhibition activities of those compounds.
- The compound **A1** possessed the best activity with IC_{50} of 2.79 μ M.
- We identified **A1** was a mixed-type xanthine oxidase inhibitor.
- Using the docking study we found **A1** could interact with the catalyze site of xanthine oxidase.

Design, synthesis and molecular modeling of aloe-emodin derivatives as potent xanthine oxidase inhibitors

Da-Hua Shi^{a,b}, Wei Huang^a, Chao Li^a, Yu-Wei Liu^c, Shi-Fan Wang^{a,*}

^a School of Ocean, Hainan University, Haikou 570228, People's Republic of China

^b School of Chemical Engineering, Huaihai Institute of Technology, Lianyungang 222005, People's Republic of China

^c Marine Economic Research Center of Jiangsu, Huaihai Institute of Technology, Lianyungang 222005, People's Republic of China

* Address for Correspondence: School of Ocean, Hainan University, Haikou 570228, People's Republic of China, E-mail: wangsf777@163.com

GRAPHIC ABSTRACT

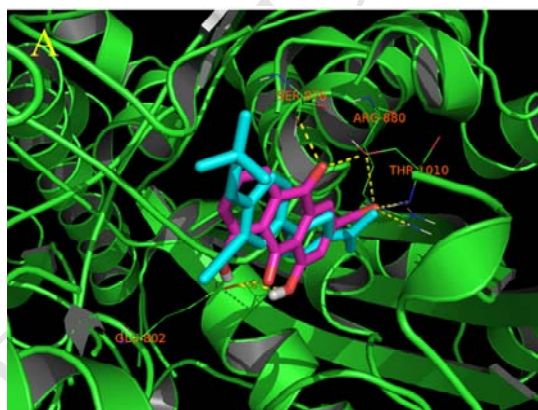
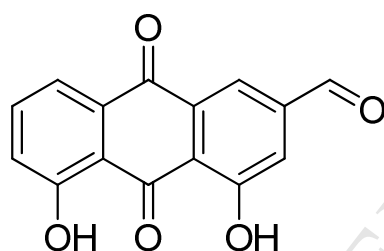
Design, synthesis and molecular modeling of aloe-emodin derivatives as potent xanthine oxidase inhibitors

Da-Hua Shi^{a,b}, Wei Huang^a, Chao Li^a, Yu-Wei Liu^c, Shi-Fan Wang^{a,*}

^a School of Ocean, Hainan University, Haikou 570228, People's Republic of China

^b School of Chemical Engineering, Huaihai Institute of Technology, Lianyungang 222005, People's Republic of China

^c Marine Economic Research Center of Jiangsu, Huaihai Institute of Technology, Lianyungang 222005, People's Republic of China



The structure of compound **A1** and the expected interaction between compound **A1** and the binding site of XDH (PDB NO. 1VDV)

* Address for Correspondence: School of Ocean, Hainan University, Haikou 570228, People's Republic of China, E-mail: wangsf777@163.com

ABSTRACT

A series of aloe-emodin derivatives were synthesized and evaluated as xanthine oxidase inhibitors. Among them, four aloe-emodin derivatives showed significant inhibitory activities against xanthine oxidase. The compound 4,5-dihydroxy-9,10-dioxo-9,10-dihydroanthracene-2-carbaldehyde (**A1**) possessed the best xanthine oxidase inhibitory activity with IC_{50} of 2.79 μ M. Lineweaver-Burk plot analysis revealed that **A1** acted as a mixed-type inhibitor for xanthine oxidase. The docking study revealed that the molecule **A1** had strong interactions with the active site of xanthine oxidase and this result was in agreement with kinetic study. Consequently, compound **A1** is a new-type candidate for further development for the treatment of gout.

Keywords: aloe-emodin; xanthine oxidase; inhibitor; gout

1. Introduction

Xanthine oxidase (XO; EC 1.17.3.2) is a key enzyme in the purine metabolic pathway[1]. There is an overwhelming acceptance that XO serum levels are increased in various pathological states like hepatitis, inflammation, ischemia-reperfusion, cancer and aging. Thus, the selective inhibition of XO may result in broad spectrum therapeutics for gout, cancer, inflammation and oxidative damage[2]. Most XO inhibitors such as allopurinol, 2-alkylhypoxanthines were purine analogs. The purine analogs could effect on the activities of purine and pyrimidine metabolism enzyme and induce life-threatening side effects[2]. Therefore, finding the non-purine compounds with potent XO-inhibition activities and fewer side effects instead of the purine analogs are in great demand[1]. As a matter of fact, some non-purine XO inhibitors, such as Y-700, a 1-phenylpyrazole derivative[3], FYX-051, a 3,5-diaryltriazole derivative[4], 2-(Pyridin-4-yl)-quinolin-4(1H)-one[5], 1-(3-(Furan-2-yl)-4,5-dihydro-5-(pyridin-4-yl)pyrazol-1-yl)ethanone[6], flavonoids[7] and curcumin[8] have been reported (Fig 1.). Recently, febuxostat, a novel non-purine XO inhibitor, has received approval for the treatment of hyperuricemia in gout patients in USA and Europe (Fig 1.)[9]. Some natural products have been reported to possess potent XO inhibitory activities [10, 11] and could be selected as the leading compounds for developing novel XO inhibitors. For example, Wu *et al.* found that a xanthone possessed good XO-inhibition activity, but the solubility of the xanthone was very poor. So they modified the compound and got series of novel xanthone

derivatives as XO inhibitors[12]. For this reason, screening and modifying of natural products is an important way to find the novel non-purine XO inhibitors.

In our previous screening of XO inhibitors from natural products, we found that the aloe-emodin (Fig. 2), an anthraquinone which is the major anthraquinone in aloe plants not only possesses antibacterial, antiviral, hepatoprotective, anticancer, laxative and anti-inflammation effects[13], but also showed the weak XO-inhibition activities with the inhibitory rate of 22.47% at the concentration of 50 $\mu\text{g/mL}$. In continuation of our previous work on finding novel non-purine XO inhibitors[11, 14], we designed and synthesized a series of aloe-emodin derivatives and tested their XO-inhibition activities.

2. Results and Discussion

2.1. Chemistry

Four series of 18 aloe-emodin derivatives **A1-A5**, **B1-B5**, **C1-C4** and **D1-D4** (Scheme 1-2) were synthesized starting from aloe-emodin (**1**) according to the methods we reported previously[15]. In series **A** (Scheme 1), the alcoholic hydroxyl of aloe-emodin (**1**) was first oxidized into the formyl group in anhydrous CH_2Cl_2 under the catalytic action of pyridinium chlorochromate (**PCC**) to obtain the compound **A1**. Then, the **A1** was modified by the condensation or the acylation with different amine to get compounds **A2** and **A3**, respectively. The compound **A1** was further oxidized to acid **A4** and **A4** was amidated to obtain **A5**. In series **B** (Scheme 1), aloe-emodin (**1**) was methylated to get **B1**. Then, **B2** was synthesized similarly with **A1**. Compounds **B3-B5** were gotten by condensation of **B2** with different amine in high yields, respectively. In series **C** (Scheme 2), the alcoholic hydroxyl group of

aloe-emodin (**1**) was initially replaced by a chlorine atom and then the quaternary ammonium was introduced into the molecule of aloe-emodin to get three derivatives of aloe-emodin **C2-C4**. In series **D** (Scheme 2), the alcoholic hydroxyl group of **B1** was initially replaced by a chlorine atom to give **D1**. Then the quaternary ammonium was introduced into the molecule of **D1** to get three derivatives of aloe-emodin **D2-D4**.

2.2. Biological activities

Anthraquinones, such as anthragallol, were reported to possess XO-inhibition activities[10]. Aloe-emodin is the major anthraquinone in aloe plants and possesses weak XO-inhibition activity. In this study, we synthesized a series of derivatives of aloe-emodin. The *in vitro* bovine XO inhibitory activities of those aloe-emodin derivatives were measured by spectrophotometry at 295 nm with the allopurinol as a reference compound[11]. The results are shown in Table 1. Among the 18 aloe-emodin derivatives, the compound **A1**, **A2**, **A3** and **C3** showed the potent XO-inhibition activities. Compared with the positive control of allopurinol ($IC_{50} = 11.23 \mu\text{M}$), the IC_{50} values of **A1**, **A2**, **A3** and **C3** are $2.79 \mu\text{M}$, $3.87 \mu\text{M}$, $8.43 \mu\text{M}$ and $18.67 \mu\text{M}$, respectively. The compound **A1** that possessed the highest XO-inhibition activity could inhibit the XO dose-dependently (Fig. 3). The Lineweaver-Burk plot (Fig. 4) revealed that compound **A1** was a mixed-type XO inhibitor. Compound **B1-B5** and compound **D1-D4** with the methylation of 4,5-hydroxyl groups exhibited significantly weak anti-XO activities compared with compounds **A1-A5** and compound **C1-C4** (Table 1). These phenomena implied that the hydroxyl groups of those aloe-emodin derivatives might play a significant role in XO-inhibition activities.

These phenomena are consistent with the findings [16, 17]. According to the XO-inhibition activities of the compound **A1-A5**, the side chains have also effects on their inhibitory activities (Table 1). The XO-inhibition activities were decreased with the increased volume of side chains. On the other hand, XO-inhibition activities of the series **C** also revealed the importance of the side chains. The compound **C3** possessed the potent XO inhibitory activity with IC_{50} of 18.67 μ M, while the compound **C2** and **C4** inhibited XO activities less than 10% inhibitory rate at the concentration of 50 μ M.

2.3. Molecular modeling

In order to understand the binding conformation of the most potent XO inhibitor **A1**, its flexible molecular docking was carried out into the active site of XO using the docking software AUTODOCK4.2 (University of California, San Francisco). The xanthine-binding site of xanthine dehydrogenase (XDH) co-crystallized with **Y-700** (PDB entry code 1VDV) was chosen as the template for docking because that both **A1** and **Y-700** are mixed-type XO inhibitors and that there is no difference between the xanthine binding-sites of XO and XDH crystal structures[18]. The docking results showed that **A1** could bind to the xanthine-binding site of XDH in a way similar to that for the **Y-700** with the binding energy of -6.99. The Fig. 5 shows the docking conformation of compound **A1** at the binding site of XDH.

The major interactions of **A1** with XDH included seven hydrogen bonds with GLU802, SER876, ARG880, and THR1010. The 4-OH and 10-carbonyl of the compound were involved in hydrogen bonding with GLU802 residue. The formyl

group of the side chain interacted with the THR1010 residue with two H-bonds and interacted with ARG880 with one H-bond. 9-carbonyl of the compound interacted with SER876 and THR1010 by H-bonds at the same time (Fig. 5). The docking results show again the free 4,5-hydroxyl groups and the formyl group in the molecule **A1** played a significant role in the XO-inhibition activities. One possible explanation for these findings is that the phenolic moiety of the compounds via hydrogen bonding and electrostatic force interacts with key amino acid residues such as ARG880, GLU1261 and THR1010[16, 19].

3. Conclusions

A series of aloe-emodin derivatives were designed, synthesized and evaluated as xanthine oxidase inhibitors. Among them, four compounds **A1**, **A2**, **A3** and **C3** showed the potent XO-inhibition activities and the IC_{50} values of **A1**, **A2**, **A3** and **C3** are 2.79 μ M, 3.87 μ M, 8.43 μ M and 18.67 μ M, respectively. Active-relationship analysis and docking study revealed that **A1** could interact with the xanthine-binding site of XO. The free 4,5-hydroxyl groups and the formyl group of side chain of the compound played significant roles for the XO-inhibition activity.

4. Experimental

4.1. Chemistry

Reaction and the resulted products were monitored by thin-layer chromatography (TLC) on the self-made pre-coated silica gel 60 F₂₅₄ plates. Spots were detected by a UV lamp visualized at 254 nm and/or 365 nm. Melting points ($^{\circ}$ C, uncorrected) were determined on a XT4 MP apparatus (Taike Corp., Beijing, China). The IR spectra were recorded on a Thermo iS10 IR spectrometer (KBr pellets) and ¹HNMR spectra

were recorded in CDCl_3 or d^6 -DMSO on a Bruker DPX400 spectrometer with TMS and solvent signals allotted as internal standards. Splitting patterns are as follows: *s*, singlet; *d*, doublet; *dd*, double doublets; *t*, triplet; *m*, multiplet. Chemical shifts are reported in δ (ppm) and coupling constants are given in Hertz. ESI mass spectra were recorded on a LCMS-IT-TOF mass spectrometer. Aloe-emodin (**1**) were purchased from Shanxi Sciphar Biotechnology Co. Ltd. (Shanxi, China) and recrystallized from DMF, m.p. 225-227 °C; $\text{IR}_{\text{vmax}}\text{cm}^{-1}$: 3131, 2367, 1672, 1628, 1572, 1400, 1288; $^1\text{HNMR}$ (d^6 -DMSO): δ = 4.60 (s, 2H, CH_2), 5.58 (s, 1H, HO- CH_2), 7.21 (s, 1H, H-C(2)), 7.31 (d, 1H, J = 8.0Hz, H-C(7)), 7.59 (s, 1H, H-C(4)), 7.62 (d, 1H, J = 7.5Hz, H-C(5)), 7.74 (dd, 1H, J_1 = 7.5Hz, J_2 = 8.0Hz, H-C(6)), 11.90 (s, 1H, HO-C(1)), 11.97 (s, 1H, HO-C(8)); HRMS (ESI): calcd for $[\text{M}+\text{H}]^+$ ($\text{C}_{15}\text{H}_{11}\text{O}_5$) m/z 271.0606, found 271.0611. XO from buttermilk, xanthine and allopurinol were purchased from Sigma-Aldrich Co.. Other reagents, all being A.R. grade, were purchased from Shanghai Chemical Reagent Company (Shanghai, China). All solvents were distilled and dried before use.

4.1.1 Synthesis of 4,5-dihydroxy-9,10-dioxo-9,10-dihydroanthracene-2-carbaldehyde (**A1**)

0.33 g (1.50 mmol) of pyridinium chlorochromate (**PCC**) was added in 200 mL of dichloromethane containing 0.27 g of compound **1** (1.0 mmol). The yielded mixture was stirred at room temperature 6 h until the reaction was accomplished. After the completion of reaction, the reaction mixture was washed with water in the separatory funnel. The dichloromethane layer was separated and the aqueous layer

was extracted twice with dichloromethane. The combined dichloromethane solutions were dried for eight hours over anhydrous sodium sulfate and then the dichloromethane was distilled off to afford a yellow solid. Recrystallization of the yellow solid from ethanol gave compound **A1** as yellow needle, yield 60 %; m.p. 208-210 °C; IR_{v_{max}}cm⁻¹: 3131, 1703, 1672, 1626, 1401, 1267; ¹HNMR (d⁶-DMSO): δ = 7.44 (d, 1H, *J* = 8.2 Hz, 1H, H-C(6)), 7.78 (s, 1H, H-C(1)), 7.84(s, 1H, H-C(3)), 7.87 (dd, 1H, *J*₁ = 8.2Hz, *J*₂ = 7.5Hz, H-C(7)), 8.15 (d, 1H, *J* = 7.5Hz, H-C(8)), 10.13 (s, 1H, CHO), 11.94 (s, 2H, OH); HRMS (ESI): calcd for [M+H]⁺ (C₁₅H₉O₅) m/z 269.0450, found 269.0453.

4.1.2. Synthesis of (*E*)-1,8-dihydroxy-3-((phenylimino)methyl)anthracene-9,10-dione (**A2**)

0.093 g (1.0 mmol) of aniline was added into a solution of compound **A1** (0.268 g, 1.0 mmol) in absolute toluene (100 mL) under stirring at 112 °C for 3 h, monitored by TLC. After the completion of reaction, the toluene of the reaction mixture was evaporated at reduced pressure to afford a yellow solid. Recrystallization of the yellow solid from ethanol gave compound **A2** as yellow needle, yield 45 %; m.p. 235-237 °C; IR_{v_{max}}cm⁻¹: 3132, 3005, 2937, 1703, 1666, 1586, 1277; ¹HNMR (d⁶-DMSO): δ=7.08-7.70 (m, 5H, on the ring of phenyl), 7.69 (d, 1H; *J*=8.0Hz, H-C(7)), 7.76 (dd, 1H, dd, *J*₁ = 8.0 Hz, *J*₂ = 7.8Hz, H-C(6)), 8.05 (d, 1H, *J* = 7.8Hz, H-C(5)), 8.23 (s, 1H, H-C(2)), 8.35 (s, 1H, H-C(4)), 8.60 (s, 1H, CH=N), 11.95 (s, 1H, HO-C(1)), 12.01 (s, 1H, HO-C(8)); HRMS (ESI): calcd for [M+H]⁺ (C₂₁H₁₄NO₄) m/z 344.0923, found 344.0929.

4.1.3. Synthesis of (3*R*,4*S*,5*S*,6*R*)-6-(acetoxymethyl)-3-((*E*)-((4,5-dihydroxy-9,10-dioxo-9,10-dihydroanthracen-2-yl)methylene)amino)tetrahydro-2-*H*-pyran-2,4,5-triyl triacetate (**A3**)

As described for **A2**, compound **A1** was treated with acetylated glucosamine to give compound **A3** as yellow needle from ethanol, yield 69 %; m.p. 231-233 °C; IR_{vmax}cm⁻¹: 3031, 2853, 1749, 1624, 1253, 1220, 761; ¹HNMR (CDCl₃): δ= 1.90-2.21(m, 12H, 4COCH₃), 3.57-5.98 (m, 7H, H-C (acetyl glucosamine)), 7.33(d, 1H, *J*=7.7Hz, H-C(6)), 7.67(s, 1H, H-C(1)), 7.72(dd, 1H, *J*₁=7.8Hz, *J*₂=8.1Hz, H-C(7)), 7.87(d, 1H, *J*=8.1Hz, H-C(8)), 8.12(s, 1H, H-C(3)), 8.30(s, 1H, CH=N), 12.01(s, 1H, OH-5), 12.04(s, 1H, OH-4); HRMS (ESI): calcd for [M+H]⁺ (C₂₉H₂₈NO₁₃) m/z 598.1561, found 598.1555.

4.1.4. Synthesis of 4,5-dihydroxy-9,10-dioxo-9,10-dihydroanthracene-2-carboxylic acid (**A4**)

A mixture of compound **1** (1 mmol, 0.27g), PCC (2 mmol, 0.45 g), DMF (100 ml) and 2mL of water were stirred at room temperature for 24h, monitored by TLC. After the completion of reaction, 100 mL of ice water was added under stirring to afford orange precipitate. The orange precipitate was filtered, washed and dried. Recrystallization of the orange precipitate from ethanol gave compound **A4** as brown acicular crystals, yield 62 %; m.p. 310-313 °C; IR_{vmax}cm⁻¹: 3432, 3059, 2930, 1695, 1628, 1270, 1192, 757; ¹HNMR (d⁶-DMSO): δ=7.58 (d, 1H, *J* = 8.2 Hz, 1H, H-C(6)), 7.85 (s, 1H, H-C(1)), 7.97 (dd, 1H, *J*₁ = 8.2Hz, *J*₂ = 7.5Hz, H-C(7)), 8.01 (s, 1H, H-C(3)), 8.45 (d, 1H, *J* = 7.5Hz, H-C(8)), 11.87 (s, 1H, HO-C(1)), 11.94 (s, 1H,

HO-C(8)), 13.90 (s, 1H, COOH); HRMS (ESI): calcd for $[M+H]^+$ ($C_{15}H_9O_6$) m/z 285.0399, found 285.0403.

4.1.5. Synthesis of (3R,4S,5S,6R)-6-(acetoxymethyl)-3-(4,5-dihydroxy-9,10-dioxo-9,10-dihydroanthracene-2-carboxamido)tetrahydro-2H-pyran-2,4,5-triyl triacetate (A5)

0.42 g (1.2 mmol) of acetylglucosamine and 0.25 g (1.2 mmol) of dicyclohexylcarbodiimide (DCC) were added into a solution of compound **A4** (0.284g, 1.0mmol) in anhydrous DMF (50 mL) under stirring at room temperature for 26 h, monitored by TLC. After the completion of reaction, the reaction mixture was filtered to remove the precipitate. 2 mL of glacial acetic acid were slowly added into the filtrate until no more precipitation was come out, standing at 4 °C for 12 h. The precipitate was filtered and then 20 mL of water was added into the filtrate under stirring to afford light yellow precipitate. The expected product was purified by column chromatography with the acetic ether-cyclohexane mixture (v:v=4:5) to give compound **A5** as pale yellow needle, yield 53 %; m.p. 239-242 °C; IR $_{\text{max}}$ cm^{-1} : 3388, 2937, 1750, 1627, 1543, 1278, 1221, 753; ^1H NMR (CDCl_3): δ =2.08-2.14(m, 12H, 4COCH₃), 3.96-5.84 (m, 7H, H-C (acetyl glucosamine)), 7.26 (d, 1H, J =8.3Hz, H-C(6)), 7.30 (s, 1H, H-C(1)), 7.63 (dd, 1H, J_1 =8.0Hz, J_2 =8.5Hz, H-C(7)), 7.65(s, 1H, H-C(3)), 7.67 (d, 1H, J =8.2Hz, H-C(8)), 7.93(s, 1H, NH), 11.73(s, 1H, OH-5), 11.79(s, 1H, OH-4); HRMS (ESI): calcd for $[M+H]^+$ ($C_{29}H_{28}NO_{14}$) m/z 614.1510, found 614.1504.

4.1.6. Synthesis of

3-(hydroxymethyl)-1,8-dimethoxyanthracene-9,10-dione (B1)

Aloe-emodin (1 mmol, 0.27 g), dimethyl sulfate (10 mmol, 1 mL) and potassium carbonate (10 mmol, 1.38 g) in 200 mL of dry acetone were refluxed for 12 h at 56 °C till the reaction was accomplished. After the completion of reaction, the yielded mixture was cooled to room temperature and filtered. The filtrate was distilled to afford a yellow solid. Recrystallization of the yellow solid from acetone gave compound **B1** as yellow needle, yield 65 %; m.p. 223-225 °C; IR/cm⁻¹: 3129, 2989, 1662, 1591, 1400, 752; ¹HNMR (d⁶-DMSO): δ = 3.91 (s, 6H, 2CH₃), 4.64 (d, *J* = 5.7 Hz, 2H, CH₂O), 5.54 (t, *J* = 5.7Hz, 1H, OH), 7.21 (1H, s, H-C(2)), 7.30 (1H, d, *J* = 8.2 Hz, H-C(7)), 7.58 (1H, s, H-C(4)), 7.61 (1H, d, *J* = 7.5Hz, H-C(5)), 7.74 (1H, dd, *J*₁ = 8.2Hz, *J*₂ = 7.5Hz, H-C(6)); HRMS (ESI): calcd for [M+H]⁺ (C₁₇H₁₅O₅) m/z 299.0919, found 299.0924.

4.1.7. Synthesis of *4,5-dimethoxy-9,10-dioxo-9,10-dihydroanthracene-2-carbaldehyde (B2)*

0.33 g (1.50 mmol) of pyridinium chlorochromate (**PCC**) was added in 250 mL of dichloromethane containing 0.30 g of compound **B1** (1.0 mmol). The yielded mixture was stirred at room temperature 3 h until the reaction was accomplished. After the completion of reaction, the reaction mixture was washed with water in the separatory funnel. The dichloromethane layer was separated and the aqueous layer was extracted twice with dichloromethane. The combined dichloromethane solutions were dried for eight hours over anhydrous sodium sulfate and then the

dichloromethane was distilled off to afford a yellow solid. Recrystallization of the yellow solid from acetone gave compound **B2**, yield 73 %; m.p. 195-197 °C; IR_{vmax}cm⁻¹: 3026, 2966, 2929, 2872, 2839, 1671, 1582, 1283; ¹HNMR (d⁶-DMSO): δ = 4.04 (s, 6H, 2CH₃), 7.26 (s, 1H, H-C(1)), 7.34 (d, 1H, *J* = 8.2 Hz, H-C(6)), 7.68 (s, 1H, H-C(3)), 7.88 (d, 1H, *J* = 7.5Hz, H-C(8)), 8.32 (dd, 1H, *J*₁ = 8.2Hz, *J*₂ = 7.5Hz, H-C(7)), 10.13 (s, 1H, CHO); HRMS (ESI): calcd for [M+H]⁺ (C₁₇H₁₃O₅) m/z 297.0763, found 297.0755.

4.1.8. Synthesis of

(E)-4,5-dimethoxy-9,10-dioxo-9,10-dihydroanthracene-2-carbaldehyde oxime (**B3**)

0.11 g (1.5 mmol) of hydroxylamine hydrochloride and 0.28 g (2.0 mmol) of anhydrous potassium carbonate were added into a solution of compound **B2** (0.296 g, 1.0 mmol) in absolute ethyl alcohol (50 mL) under stirring at 65°C for 0.5 h, monitored by TLC. After the completion of reaction, the reaction mixture was filtered to remove the solid of inorganic salt and the solvent was evaporated at reduced pressure to afford a yellow solid. Recrystallization of the yellow solid from ethanol gave compound **B3** as yellow needle, yield 65 %; m.p. 247-249 °C; IR_{vmax}cm⁻¹: 3315, 3059, 2929, 1659, 1587, 1283, 1237, 753; ¹HNMR (d⁶-DMSO): δ=3.94 (s, 6H, 2CH₃), 7.53 (s, 1H, H-C(1)), 7.66 (d, 1H, *J* = 8.2 Hz, H-C(6)), 7.69 (s, 1H, H-C(3)), 7.74 (d, 1H, *J* = 7.5Hz, H-C(8)), 7.92 (dd, 1H, *J*₁ = 8.2Hz, *J*₂ = 7.5Hz, H-C(7)), 8.31 (s, 1H, CH), 11.78 (s, 1H, NOH); HRMS (ESI): calcd for [M+H]⁺ (C₁₇H₁₄NO₅) m/z 312.0872, found 312.0879.

4.1.9. Synthesis of

(E)-1,8-dimethoxy-3-((phenylimino)methyl)anthracene-9,10-dione (**B4**)

As described for **A2**, compound **B2** was treated with aniline to give compound **B4** as orange needle from ethanol, yield 70 %; m.p. 225-228 °C; IR_{vmax}cm⁻¹: 3092, 2927, 1666, 1586, 1277, 1235, 788; ¹HNMR (CDCl₃): δ = 4.12 (s, 6H, 2CH₃), 7.18-7.70(m, 5H, on the ring of phenyl), 7.65 (d, 1H; *J* = 8.1Hz, H-C(7)), 7.71 (dd, 1H, dd, *J*₁ = 8.1Hz, *J*₂ = 7.8Hz, H-C(6)), 8.03 (d, 1H, *J* = 7.5Hz, H-C(5)), 8.18 (s, 1H, H-C(2)), 8.31 (s, 1H, H-C(4)), 8.57 (s, 1H, CH=N); HRMS (ESI): calcd for [M+H]⁺ (C₂₃H₁₈NO₄) m/z 372.1236, found 372.1230.

4.1.10. Synthesis of

(E)-3-(hydrazonomethyl)-1,8-dimethoxyanthracene-9,10-dione (**B5**)

As described for **B3**, compound **B2** was treated with hydrazine sulfate to give compound **B4** as bright yellow needle from ethanol, yield 74 %; m.p. 280 °C (dec.); IR_{vmax}cm⁻¹: 3062, 2958, 1668, 1590, 1286, 1235, 748; ¹HNMR (CDCl₃): δ = 3.54(s, 2H, NH₂), 4.03 (s, 6H, 2CH₃), 7.33 (d, 1H; *J* = 8.1Hz, H-C(7)), 7.67 (dd, 1H, dd, *J*₁ = 8.1Hz, *J*₂ = 7.8Hz, H-C(6)), 7.86 (d, 1H, *J* = 7.4Hz, H-C(5)), 7.95 (s, 1H, H-C(2)), 8.16 (s, 1H, H-C(4)), 8.73(s, 1H, CH=N); HRMS (ESI): calcd for [M+H]⁺ (C₁₇H₁₅N₂O₄) m/z 311.1032, found 311.1038.

4.1.11. Synthesis of

3-(chloromethyl)-1,8-dihydroxyanthracene-9,10-dione (**C1**)

2 mL of thionyl chloride was slowly added into a solution of compound **A1** (0.27 g, 1.0 mmol) in anhydrous DMF (20 mL) under stirring at room temperature for 26 h,

monitored by TLC. After the completion of reaction, 60 mL of ice water was added under stirring to afford orange precipitate. The orange precipitate was filtered, washed and dried. Recrystallization of the orange precipitate from ethanol gave compound **C1** as yellow needle, yield 55 %; m.p. 177-178 °C; IR_{v_{max}}cm⁻¹: 3426, 3041, 1672, 1627, 1569, 1478, 1454, 1422, 1381, 1276; ¹HNMR (CDCl₃): δ = 4.62 (s, 2H, CH₂), 7.31 (s, 1H, H-C(4)), 7.35 (d, 1H, *J* = 8.0Hz, H-C(7)), 7.71 (dd, 1H, *J*₁ = 7.5Hz, *J*₂ = 8.0Hz, H-C(6)), 7.85 (s, 1H, H-C(2)), 7.86 (d, 1H, *J* = 7.5Hz, H-C(5)), 12.04 (s, 1H, HO), 12.07 (s, 1H, HO); HRMS (ESI): calcd for [M+H]⁺ (C₁₅H₁₀ClO₄) m/z 289.0268, found 289.0265.

4.1.12. Synthesis of

1-((4,5-dihydroxy-9,10-dioxo-9,10-dihydroanthracen-2-yl)methyl)pyridi-1-ium chloride (C2)

1 mL of dry pyridine was slowly added into a solution of compound **C1** (0.29 g, 1.0 mmol) in anhydrous CHCl₃ (50 mL) under stirring at room temperature. The reaction mixture was allowed to stand at room temperature for 2 weeks and orange crystals were formed at the bottom of the vessel, yield 60 %; m.p. 235 °C (dec.); IR_{v_{max}}cm⁻¹: 3418, 3059, 2955, 1629, 1563, 1280, 1214, 755; ¹HNMR (D₂O): δ = 5.92 (s, 2H, CH₂), 7.19 (d, 1H, *J* = 8.4Hz, H-C (6)), 7.24(s, 1H, H-C (1)), 7.43(d, 1H, *J* = 7.4Hz, H-C (8)), 7.46(s, 1H, H-C (3)), 7.62 (dd, 1H, *J*₁ = 8.2Hz, *J*₂ = 7.8Hz, H-C (7)), 8.20(d, 2H, *J* = 6.8Hz, H-C (pyridyl-3',5')), 8.70 (dd, 1H, *J*₁ = 7.9Hz, *J*₂ = 7.9Hz, H-C (pyridyl-4')), 9.02 (d, 2H, *J* = 5.6Hz, H-C (pyridyl-2',6')), 11.81 (s, 2H, 2OH); HRMS (ESI): calcd for [M-Cl]⁺ (C₂₀H₁₄NO₄) m/z 332.0943, found 332.0941.

4.1.13. Synthesis of

1-(4,5-dihydroxy-9,10-dioxo-9,10-dihydroanthracen-2-yl)-N,N,N-trimethylmethanaminium chloride (**C3**)

As described for **C2**, compound **C1** was treated with trimethylamine to give compound **C3** as yellow needle, yield 65 %; m.p. 230 °C (dec.); IR_{vmax}cm⁻¹: 3413, 3022, 2957, 1629, 1477, 1285, 1200, 752; ¹HNMR (D₂O): δ = 3.20(s, 9H, CH₃), 4.95 (s, 2H, CH₂), 7.19(d, 1H, *J* = 8.4Hz, H-C (6)), 7.40(s, 1H, H-C (3)), 7.44(d, 1H, *J* = 7.5Hz, H-C (8)), 7.60(s, 1H, H-C (1)), 7.64(dd, 1H, *J*₁ = 8.2Hz, *J*₂ = 7.8Hz, H-C (7)), 12.05 (s, 2H, 2OH); HRMS (ESI): calcd for [M-Cl]⁺ (C₁₈H₁₈NO₄) m/z 312.1256, found 312.1257.

4.1.14. Synthesis of

N-((4,5-dihydroxy-9,10-dioxo-9,10-dihydroanthracen-2-yl)methyl)-N,N-dimethylbenzenaminium chloride (**C4**)

As described for **C2**, compound **C1** was treated with N,N-dimethylaniline to give compound **C4** as orange needle, yield 63 %; m.p. 182 °C (dec.); IR_{vmax}cm⁻¹: 3414, 3008, 2928, 1636, 1489, 1271, 1215, 746; ¹HNMR (D₂O): δ = 3.52 (s, 6H, 2NCH₃), 5.02 (s, 2H, CH₂), 6.97 (s, 1H, H-C (1)), 7.05 (d, 1H, *J* = 8.4Hz, H-C (6)), 7.20 (s, 1H, H-C (3)), 7.28 (d, 1H, *J* = 7.4Hz, H-C (8)), 7.35 (dd, 1H, *J*₁ = 8.2Hz, *J*₂ = 7.8Hz, H-C (7)), 7.70-8.53 (m, 5H, H-C (benzene ring)), 12.05 (s, 2H, 2OH); HRMS (ESI): calcd for [M-Cl]⁺ (C₂₃H₂₀NO₄) m/z 374.1392, found 374.1396.

4.1.15. Synthesis of

3-(Chloromethyl)-1,8-dimethoxyanthracene-9,10-dione (**D1**)

As described for **C1**, compound **B1** was chloridized with thionyl chloride to give compound **D1** as yellow needle from acetone, yield 80%; m.p. 179-182 °C; IR_{vmax}cm⁻¹: 3004, 2932, 1666, 1586, 1284, 1237, 712; ¹H NMR (CDCl₃): d = 4.01 (s, 3H, CH₃), 4.04 (s, 3H, CH₃), 4.65 (s, 2H, CH₂), 7.30 (d, 1H, J = 8.3 Hz, H-C(7)), 7.34 (s, 1H, HC(2)), 7.65 (dd, 1H, J₁ = 7.8 Hz, J₂ = 8.3 Hz, H-C(6)), 7.83 (s, 1H, HC(4)), 7.84 (d, 1H, J = 7.8 Hz, H-C(5)); HRMS (ESI): calcd for [M+H]⁺ (C₁₇H₁₄ClO₄) m/z 317.0581, found 317.0585.

4.1.16. Synthesis of

1-((4,5-Dimethoxy-9,10-dioxo-9,10-dihydroanthracen-2-yl)methyl)pyridin-1-ium chloride (D2)

1 ml of dry pyridine was slowly added into a solution of compound **D1** (0.32 g, 1.0 mmol) in anhydrous CHCl₃ (50 mL) under stirring at room temperature. The reaction mixture was allowed to stand at room temperature for 2 weeks and yellow crystals were formed at the bottom of the vessel, yield 73%; m.p. 168 °C (dec); IR_{vmax} cm⁻¹: 3219, 3047, 1663, 1587, 1277, 1239, 741; ¹H NMR (D₂O): d = 3.94 (s, 3H, CH₃-5), 3.96 (s, 3H, CH₃-4), 5.93 (s, 2H, CH₂), 7.47 (d, 1H, J = 8.6 Hz, H-C (6)), 7.50 (d, 1H, J = 6.7 Hz, H-C (8)), 7.52 (s, 1H, H-C (1)), 7.57 (s, 1H, H-C (3)), 7.68 (dd, 1H, J₁ = 8.1 Hz, J₂ = 8.0 Hz, H-C (7)), 8.16 (d, 2H, J = 6.8 Hz, H-C (pyridyl-3',5')), 8.66 (dd, 1H, J₁ = 7.9 Hz, J₂ = 7.9 Hz, H-C (pyridyl-4')), 8.99 (d, 2H, J = 5.6 Hz, H-C (pyridyl-2',6')); HRMS (ESI): Calcd for [M-Cl]⁺(C₂₂H₁₈NO₄) m/z 360.1236, found 360.1124.

4.1.17. Synthesis of

1-(4,5-Dimethoxy-9,10-dioxo-9,10-dihydroanthracen-2-yl)-N,N,N-trimethylmethanaminium chloride (D3)

As described for **D2**, compound **D1** was treated with trimethylamine to give

compound **D3** as yellow needle, yield 74%; m.p. 219 °C (dec); IR ν_{\max} cm^{-1} : 3009, 2962, 1661, 1591, 1282, 1235, 746; ^1H NMR (D_2O): d = 3.20 (s, 9H, CH_3), 3.90 (s, 6H, 2OCH_3), 4.52 (s, 2H, CH_2), 7.30 (d, 1H, $J = 7.5$ Hz, H-C (6)), 7.38 (d, 1H, $J = 8.3$ Hz, H-C 8)), 7.47 (s, 1H, H-C (3)), 7.57 (s, 1H, H-C (1)), 7.58 (dd, 1H, $J_1 = 6.8$ Hz, $J_2 = 9.3$ Hz, H-C (7)); HRMS (ESI): Calcd for $[\text{M}-\text{Cl}]^+$ ($\text{C}_{20}\text{H}_{22}\text{NO}_4$) m/z 340.1549, found 340.1560.

4.1.18. Synthesis of

N-((4,5-Dimethoxy-9,10-dioxo-9,10-dihydroanthracen-2-yl)methyl)-*N,N*-dimethylbenzenaminium chloride (**D4**)

As described for **D2**, compound **D1** was treated with *N,N*-dimethylaniline to give compound **D4** as yellow needle, yield 70%; m.p. 161 °C (dec); IR ν_{\max} cm^{-1} : 3005, 2963, 1674, 1585, 1285, 1241, 751; ^1H NMR (D_2O): d = 3.53 (s, 6H, 2NCH_3), 3.74 (s, 6H, 2OCH_3), 4.96 (s, 2H, CH_2), 6.64 (s, 1H, H-C (1)), 6.81 (d, 1H, $J = 7.5$ Hz, H-C (6)), 6.88 (s, 1H, H-C (3)), 7.12 (d, 1H, $J = 8.1$ Hz, HC (8)), 7.24 (dd, 1H, $J_1 = 8.3$ Hz, $J_2 = 7.7$ Hz, H-C (7)), 7.64-7.73 (m, 5H, H-C (benzene ring)); HRMS (ESI): Calcd for $[\text{M}-\text{Cl}]^+$ ($\text{C}_{25}\text{H}_{24}\text{NO}_4$) m/z 402.1705, found 402.1699.

4.2 Assay of the *in vitro* XO inhibitory activity

The XO activity with xanthine as the substrate was measured at 25 °C, according to the protocol of Kong and others[20]. The reaction mixture contained 650 μL of 50 mM K_2HPO_4 buffer (pH 7.8), 200 μL of 84.8 $\mu\text{g}/\text{mL}$ xanthine in 50 mM K_2HPO_4 buffer, and 50 μL of the various concentrations of tested compounds, which were dissolved in DMSO. The reaction was started by addition of 100 μL of XO (25 mU/mL) and was monitored for 6 min at 295 nm. The XO activity was expressed as the change in absorbance per minute at 295nm.

4.2. Molecular Modeling Evaluations[21, 22]

The pdb structure of xanthine dehydrogenase (XDH) co-crystallized with **Y-700** (PDB entry code 1VDV) was obtained from the Protein Data Bank. The 3D structure of compound **A1** was constructed utilizing ChemBioOffice 2008 and optimized according to the standard protocol of ChemBio 3D.

Docking studies were carried out using the AUTODOCK 4.2.3 program. Using ADT[23], Polar hydrogen atoms were added to amino acid residues and Gasteiger charges were assigned to all atoms of the enzyme. The resulting enzyme structure was used as an input for the AUTOGRID program. AUTOGRID performed a precalculated atomic affinity grid maps for each atom type in the ligand plus an electrostatics map and a separate desolvation map present in the substrate molecule. All maps were calculated with 0.375 Å spacing between grid points. The centre of the grid box was placed at the centre of the **Y-700**. The dimensions of the active site box were set at 50 × 50 × 50 Å.

Flexible ligand docking was performed for the compound. Docking calculations were carried out using the Lamarckian genetic algorithm (LGA) and all parameters were the same for each docking. A population of random individuals (population size: 150), a medium number of 2,500,000 energy evaluations, a maximum number of generations of 27,000 was used. At the end of docking procedure (100 docking runs), the resulting positions were clustered according to a root mean square criterion of 0.5 Å.

Acknowledgment

The financial support of the Natural Science Foundation of P.R. China (grated No: 21162006), Postdoctoral Science Foundation of China (grated No: 2012M521659) and Collegiate Natural Science Fund of Jiangsu Province (12KJB350001) are gratefully acknowledged.

References

- [1] S. Wang, J. Yan, J. Wang, J. Chen, T. Zhang, Y. Zhao, M. Xue, Synthesis of some 5-phenylisoxazole-3-carboxylic acid derivatives as potent xanthine oxidase inhibitors, *Eur J Med Chem*, 45 (2010) 2663-2670.
- [2] K. Nepali, A. Agarwal, S. Sapra, V. Mittal, R. Kumar, U.C. Banerjee, M.K. Gupta, N.K. Satti, O.P. Suri, K.L. Dhar, N-(1,3-Diaryl-3-oxopropyl)amides as a new template for xanthine oxidase inhibitors, *Bioorg. Med. Chem.*, 19 (2011) 5569-5576.
- [3] S. Ishibuchi, H. Morimoto, T. Oe, T. Ikebe, H. Inoue, A. Fukunari, M. Kamezawa, I. Yamada, Y. Naka, Synthesis and structure-activity relationships of 1-Phenylpyrazoles as xanthine oxidase inhibitors, *Bioorg. Med. Chem. Lett.*, 11 (2001) 879-882.
- [4] K. Okamoto, K. Matsumoto, R. Hille, B.T. Eger, E.F. Pai, T. Nishino, The crystal structure of xanthine oxidoreductase during catalysis: implications for reaction mechanism and enzyme inhibition, *Proc. Natl. Acad. Sci. U.S.A.*, 101 (2004) 7931-7936.
- [5] R. Dhiman, S. Sharma, G. Singh, K. Nepali, P.M. Singh Bedi, Design and synthesis of aza-flavones as a new class of xanthine oxidase inhibitors, *Arch. Pharm. Chem. Life Sci.*, 346 (2013) 7-16.
- [6] K. Nepali, G. Singh, A. Turan, A. Agarwal, S. Sapra, R. Kumar, U.C. Banerjee, P.K. Verma, N.K. Satti, M.K. Gupta, O.P. Suri, K.L. Dhar, A rational approach for the design and synthesis of 1-acetyl-3,5-diaryl-4,5-dihydro(1H)pyrazoles as a new class of potential non-purine xanthine oxidase inhibitors, *Bioorg. Med. Chem.*, 19 (2011) 1950-1958.
- [7] D.E.C. Van Hoorn, R.J. Nijveldt, P.A.M. Van Leeuwen, Z. Hofman, L. M'Rabet, D.B.A. De Bont, K. Van Norren, Accurate prediction of xanthine oxidase inhibition based on the structure of flavonoids, *Eur. J. Pharmacol.*, 451 (2002) 111-118.
- [8] L. Shen, H.F. Ji, Insights into the inhibition of xanthine oxidase by curcumin, *Bioorg. Med. Chem. Lett.*, 19 (2009) 5990-5993.
- [9] M.K. Reinders, T.L. Jansen, Management of hyperuricemia in gout: focus on febuxostat, *Clin Interv Aging*, 5 (2010) 7-18.

- [10] F. Borges, E. Fernandes, F. Roleira, Progress towards the discovery of xanthine oxidase inhibitors, *Curr. Med. Chem.*, 9 (2002) 195-217.
- [11] R.H. Jiao, H.M. Ge, D.H. Shi, R.X. Tan, An Apigenin-Derived Xanthine Oxidase Inhibitor from *Palhinhaea cernua*, *J. Nat. Prod.*, 69 (2006) 1089-1091.
- [12] L. Hu, H. Hu, W. Wu, X. Chai, J. Luo, Q. Wu, Discovery of novel xanthone derivatives as xanthine oxidase inhibitors, *Bioorg. Med. Chem. Lett.*, 21 (2011) 4013-4015.
- [13] M.Y. Park, H.J. Kwon, M.K. Sung, Evaluation of Aloin and Aloe-Emodin as Anti-Inflammatory Agents in Aloe by Using Murine Macrophages, *Biosci., Biotechnol., Biochem.*, 73 (2009) 828-832.
- [14] Z.L. You, D.H. Shi, C. Xu, Q. Zhang, H.L. Zhu, Schiff base transition metal complexes as novel inhibitors of xanthine oxidase, *Eur J Med Chem*, 43 (2008) 862-871.
- [15] D.H. Shi, W. Huang, C. Li, L.T. Wang, S.F. Wang, Synthesis, biological evaluation and molecular modeling of aloe-emodin derivatives as new acetylcholinesterase inhibitors, *Bioorg. Med. Chem.*, 21 (2013) 1064-1073.
- [16] M. Leigh, D.J. Raines, C.E. Castillo, A.K. Duhme-Klair, Inhibition of Xanthine Oxidase by Thiosemicarbazones, Hydrazones and Dithiocarbazates Derived from Hydroxy-Substituted Benzaldehydes, *ChemMedChem*, 6 (2011) 1107-1118.
- [17] Y.T. Tung, S.T. Chang, Inhibition of Xanthine Oxidase by *Acacia confusa* Extracts and Their Phytochemicals, *J. Agric. Food Chem.*, 58 (2010) 781-786.
- [18] B.R. C, A. Kulkarni-Almeida, K.V. Katkar, S. Khanna, U. Ghosh, A. Keche, P. Shah, A. Srivastava, V. Korde, K.V. Nemmani, N.J. Deshmukh, A. Dixit, M.K. Brahma, U. Bahirat, L. Doshi, R. Sharma, H. Sivaramakrishnan, Identification of novel isocytosine derivatives as xanthine oxidase inhibitors from a set of virtual screening hits, *Bioorg. Med. Chem.*, 20 (2012) 2930-2939.
- [19] Y.C. Chang, F.W. Lee, C.S. Chen, S.T. Huang, S.H. Tsai, S.H. Huang, C.M. Lin, Structure-activity relationship of C6-C3 phenylpropanoids on xanthine oxidase-inhibiting and free radical-scavenging activities, *Free Radic. Biol. Med.*, 43 (2007) 1541-1551.
- [20] L.D. Kong, Y. Zhang, X. Pan, R.X. Tan, C.H.K. Cheng, Inhibition of xanthine oxidase by liquiritigenin and isoliquiritigenin isolated from *Sinofranchetia chinensis*, *Cell. Mol. Life Sci.*, 57 (2000) 500-505.
- [21] J.W. Yan, Y.P. Li, W.J. Ye, S.B. Chen, J.Q. Hou, J.H. Tan, T.M. Ou, D. Li, L.Q. Gu, Z.S. Huang, Design, synthesis and evaluation of isaindigotone derivatives as dual inhibitors for acetylcholinesterase and amyloid beta aggregation, *Bioorg. Med. Chem.*, 20 (2012) 2527-2534.
- [22] S. Gupta, L.M. Rodrigues, A.P. Esteves, A.M.F. Oliveira-Campos, M.S.o.J. Nascimento, N. Nazareth, H. Cidade, M.P. Neves, E. Fernandes, M. Pinto, N.M.F.S.A. Cerqueira, N.r. Brã;s, Synthesis of N-aryl-5-amino-4-cyanopyrazole derivatives as potent xanthine oxidase inhibitors, *Eur J Med Chem*, 43 (2008) 771-780.
- [23] M.F. Sanner, Python: a programming language for software integration and development, *J. Mol. Graphics Model.*, 17 (1999) 57-61.

Figure Captions

Figure 1. Some reported non-purine XO inhibitors.

Figure 2. Chemical structure of aloe-emodin.

Figure 3. The inhibition of compound A1 on the XO. Values are means \pm SD, n=3.

Figure 4. Steady-state inhibition of XO by A1. Lineweaver-Burk plot of reciprocal of initial velocities versus reciprocal of five fixed xanthine concentrations (20, 30, 40, 60 and 80 $\mu\text{g/mL}$) in the absence (\blacklozenge) and presence of A1 at 1.4 μM (\blacksquare), 2.8 μM (\blacktriangle) and 5.6 μM (\bullet).

Figure 5. A close view of the potential interaction between compound A1 and the binding site of XDH (PDB NO. 1VDV). A: Binding interactions of A1 in the catalytic site of XDH. The blue molecular was Y-700; B: Compound A1 docked into the binding site of XDH. The blue molecular was Y-700.

Scheme Captions

Scheme 1. Synthetic pathway for compounds A1-A5 and B1-B5

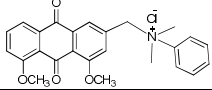
Scheme 2. Synthetic pathway for compounds C1-C4 and D1-D4

Table Caption

Table 1. The XO-inhibition activities of aloe-emodin derivatives

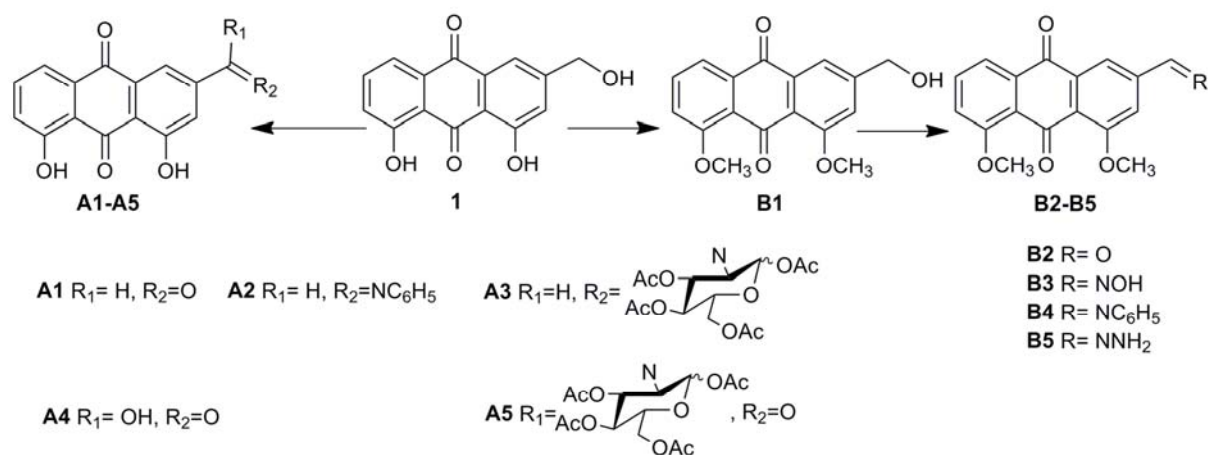
Table 1. The XO-inhibition activities of aloe-emodin derivatives

Compound	Structures	Inhibition	
		Inhibition (%) ^a	IC ₅₀ (μM)
1		22.46	-
A1		93.27	2.79 ± 0.64
A2		94.55	3.87 ± 0.35
A3		93.38	8.43 ± 1.81
A4		3.63	-
A5		7.20	-
B1		9.77	-
B2		36.47	-
B3		n.a. ^b	-
B4		17.47	-
B5		n.a.	-
C1		18.45	-
C2		n.a.	-
C3		68.85	18.67 ± 2.01
C4		n.a.	-
D1		14.26	-
D2		n.a.	-
D3		n.a.	-

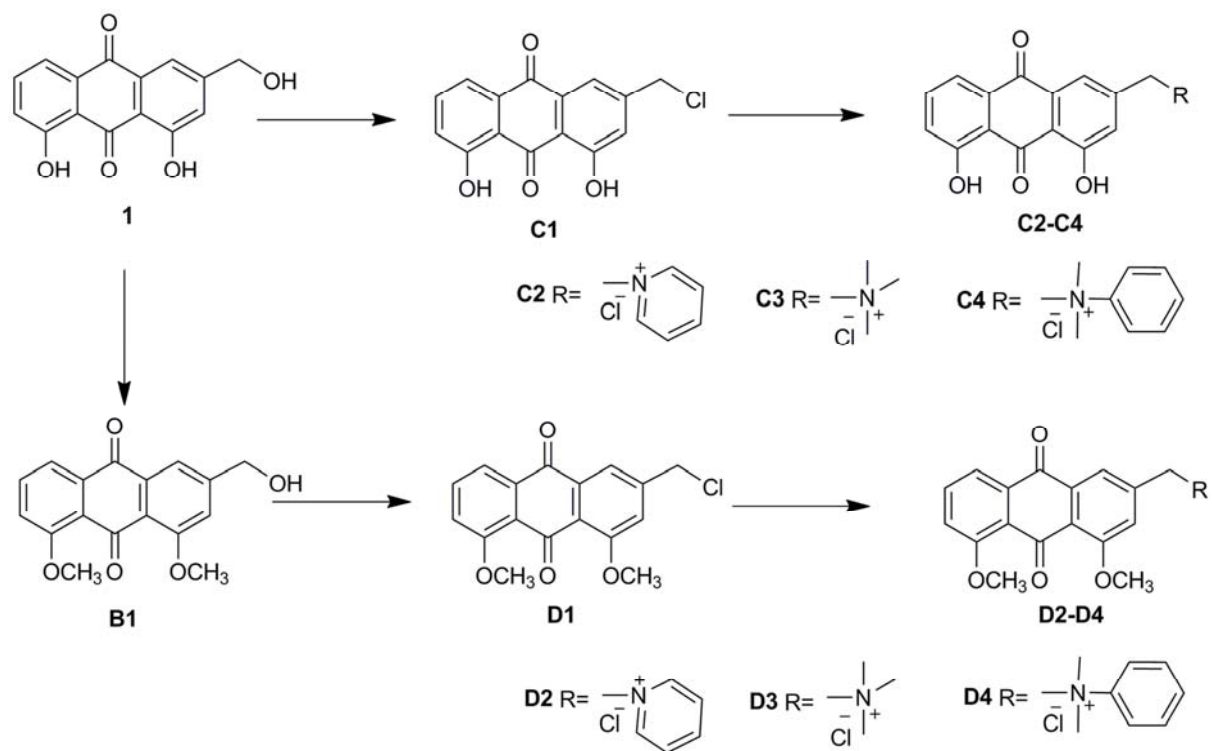
D4		n.a.
Allopurinol		11.23 ± 0.11

^aThe inhibition activities of the compounds at the concentration of 50 μM.

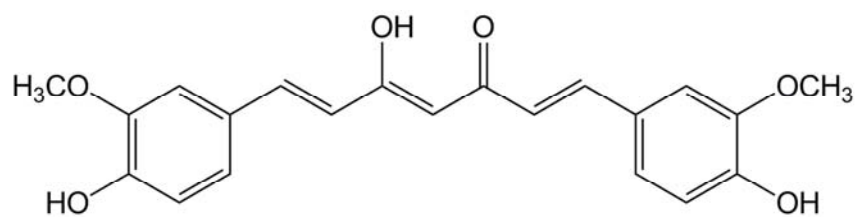
^b n.a.:not active(less than 10% inhibition at 50 μM).



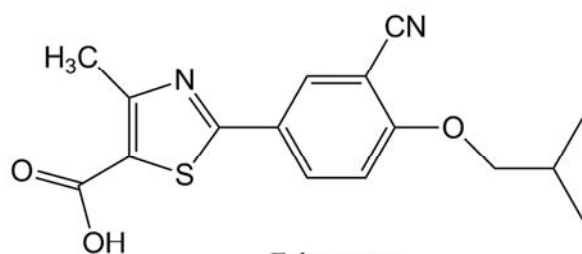
Scheme 1



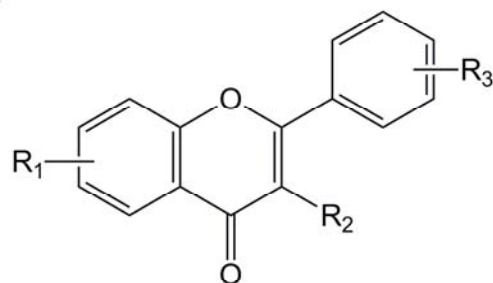
Scheme 2



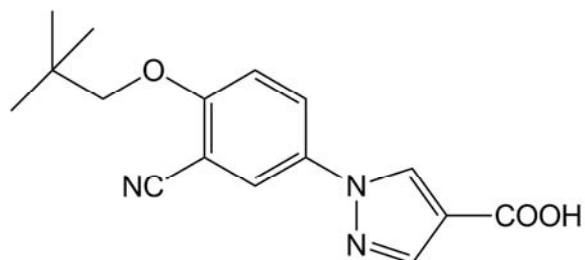
Curcumin



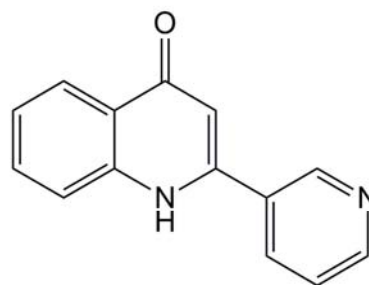
Febuxostat



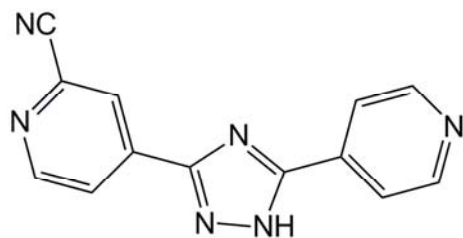
Flavonoids



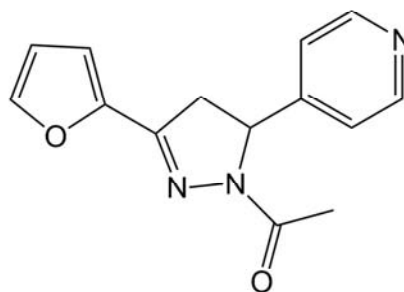
Y-700



2-(Pyridin-4-yl)-quinolin-4(1H)-one

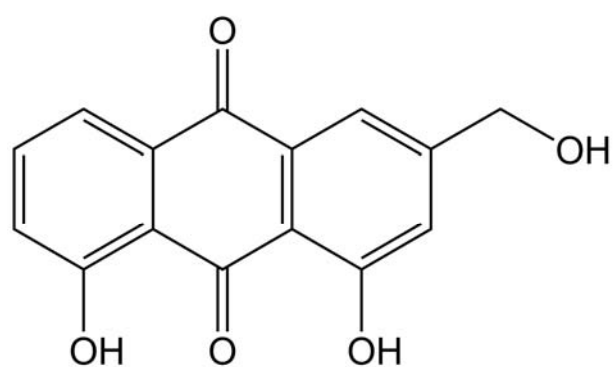


FYX-051



1-(3-(Furan-2-yl)-4,5-dihydro-5-(pyridin-4-yl)pyrazol-1-yl)ethanone

Figure 2



ACCEPTED MANUSCRIPT

Figure 3

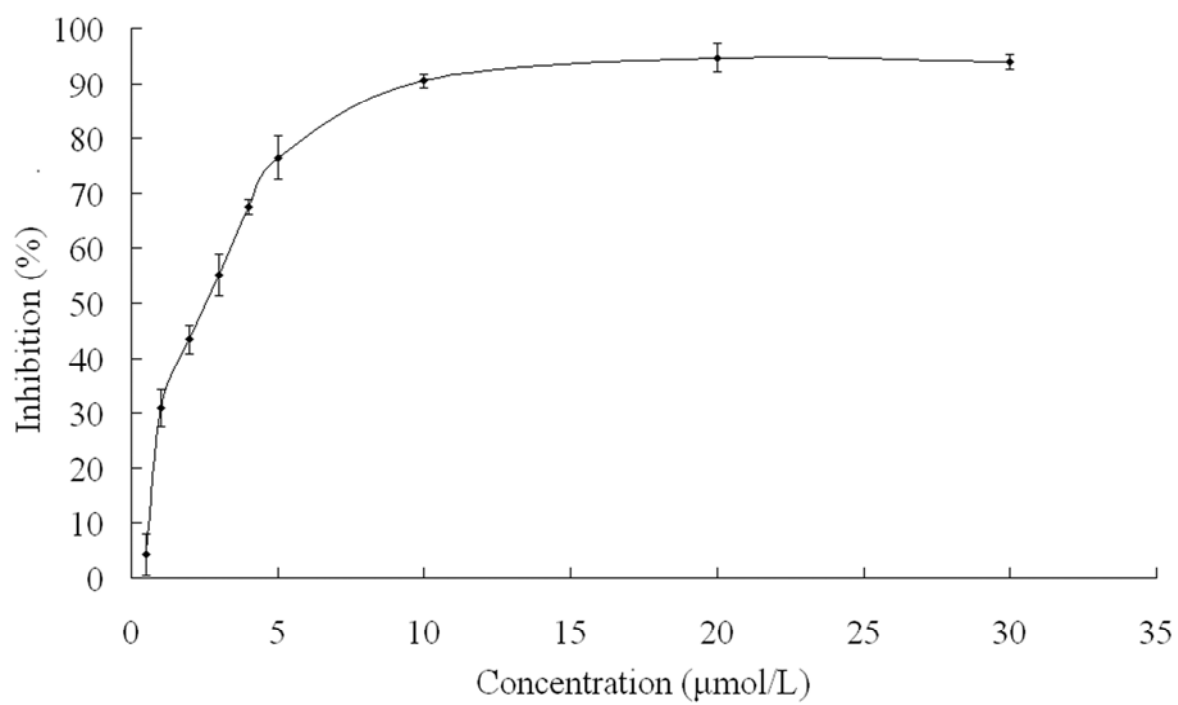


Figure 4

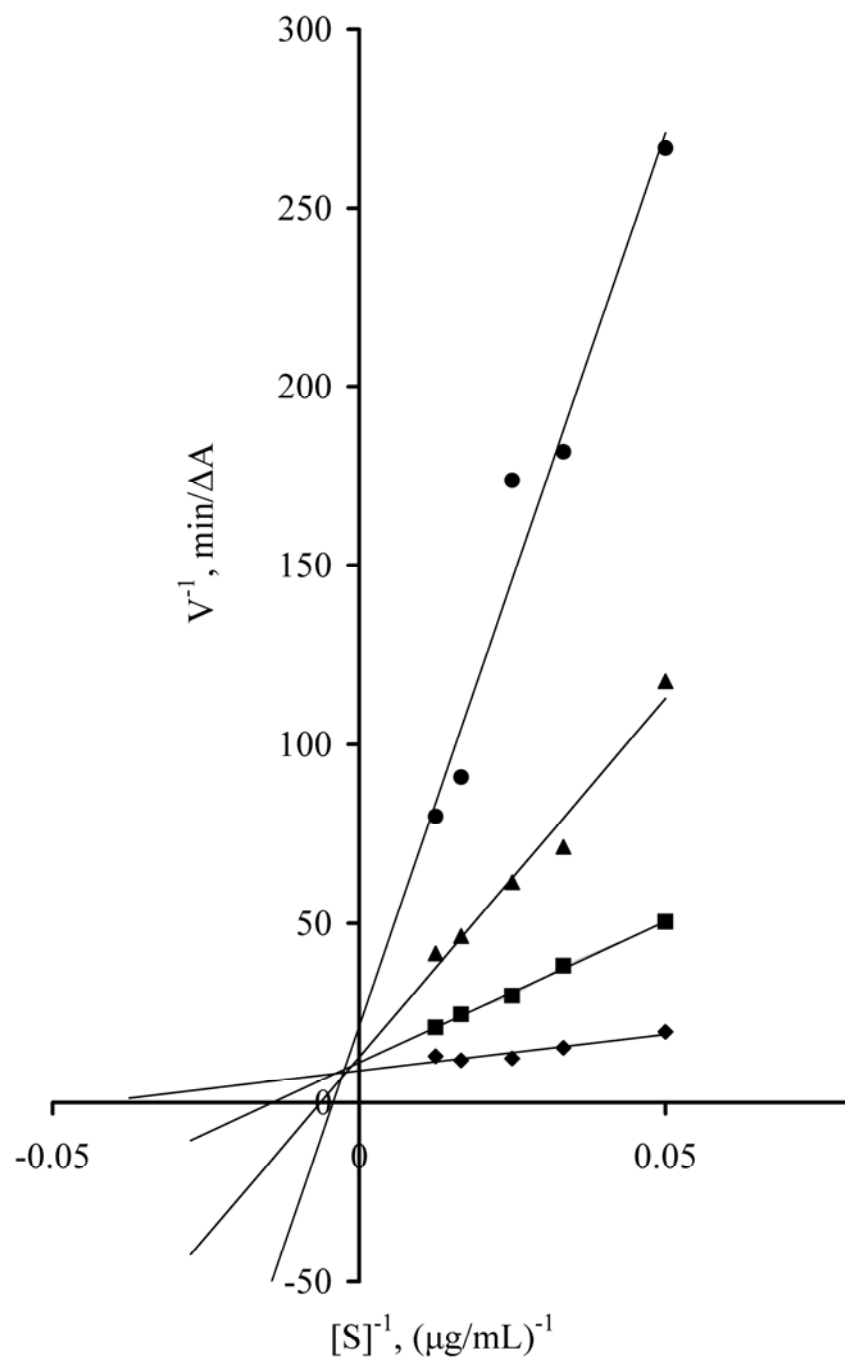
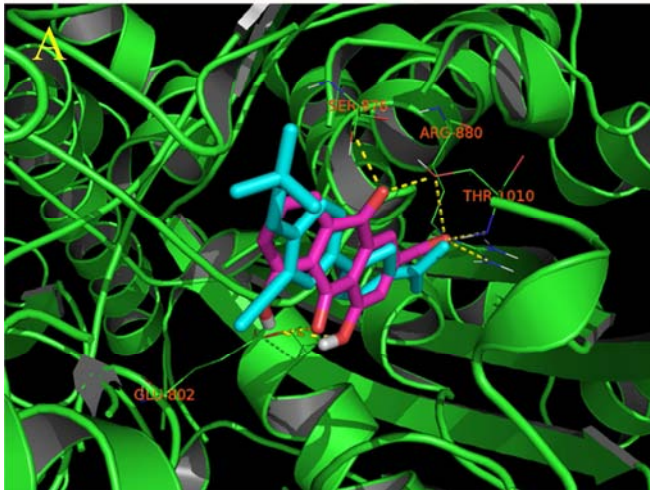
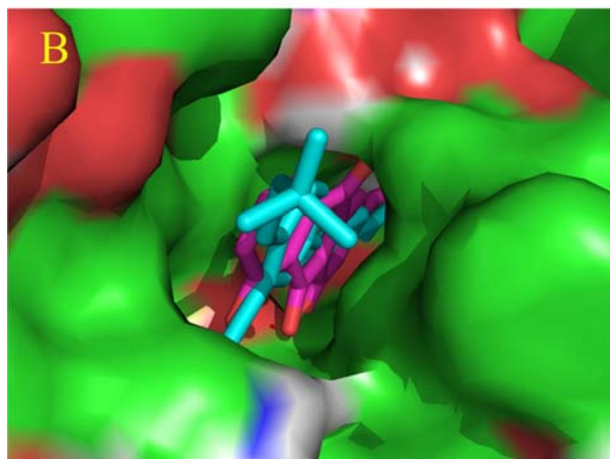


Figure 5A



ACCEPTED MANUSCRIPT

Figure 5B



ACCEPTED MANUSCRIPT